J Mater Sci (2007) 42:8158–8162
DOI 10.1007/s10853-007-1704-9

N and p doped poly(3,4-ethylenedioxythiophene) electrode materials for symmetric redox supercapacitors

D. Krishna Bhat · M. Selva Kumar

Received: 22 September 2006 / Accepted: 16 March 2007 / Published online: 12 June 2007

Abstract A symmetric redox supercapacitor has been fabricated based on n and p doped Poly(3,4-ethylenedioxythiophene)(PEDOT) coated on stainless steel (SS) electrodes. The characterization and performance of the supercapacitor has been studied by FTIR, Cyclic Voltammetry and AC Impedance spectroscopy. The supercapacitor showed a maximum specific capacitance of 121 F g^{-1} at a scan rate of 10 mV s^{-1}. The time constant calculated for the supercapacitor through the active–reactive power behavior measurement was 12 milliseconds indicating the suitability of the system for efficient use at low frequency range.

Introduction

Conducting polymers as electrode materials for redox supercapacitors have shown several advantages due to the fast charge–discharge kinetics, low cost, suitable morphology and fast doping- un doping processes [1–4]. The versatility of these conducting polymers enables different redox supercapacitor configurations such as type I, II and III [5]. Among these the type III configuration is the most favourable in terms of energy and power density for electric vehicle applications. But these advantages are offset by the difficulty of obtaining polymer electrodes that can be n-doped in a truly efficient way. Polypyrrole cannot be n-doped because the injection of negative charges would require potentials so negative as to be incompatible with polymer and electrolyte stability. Polythiophene, on the other hand with a smaller band gap allows both p- and n-doping with several salt solvent combinations having a wide electrochemical stability window and hence the p- and n- dopable polythiophene derivatives as electrodes have been typically used to obtain high energy and power density for electrochemical supercapacitors [6–10]. However to the best of our knowledge there are no reports in the literature on supercapacitors based on n- and p- doped poly(3,4-ethylenedioxythiophene)(PEDOT). Hence we report herein the preliminary studies on the preparation, characterization and performance of a symmetric redox supercapacitor based on n- and p- doped PEDOT electrodeposited on stainless steel (SS) electrodes.

D. K. Bhat (✉) · M. Selva Kumar
Department of Chemistry, National Institute of Technology Karnataka Surathkal, Srinivasnagar, 575025 Mangalore, India
e-mail: denthaje@gmail.com; kishan@nitk.ac.in

Experimental

All the chemicals used in the study were of analar grade. Tertrabutyl ammonium perchlorate and 3,4-ethylenedioxythiophene were purchased from Aldrich and used as such. Acetonitrile was purified by distillation and stored over 3A° molecular sieves.

Cyclic Voltammetry experiments were conducted with AUTOLAB 30 from Eco-Chemie, The Netherlands. A three electrode system was employed with Ag/AgCl as reference electrode for both p and n-doping. Stainless steel (SS) electrodes were used as both working and counter electrodes. The active material was directly deposited on to the SS electrodes. For both p- and n- doping of the electrodes, 0.1 M Tetrabutylammoniumperchlorate ($[C_4H_5]_4N^+ ClO_4^-$) in acetonitrile was used as the electrolyte. The electrode responses were analyzed by AC Impedance spectroscopy in the frequency range of 0.1–10^6 Hz. FTIR

measurements were conducted using a NICOLET AVATAR 330 FTIR spectrometer. In the fabrication of the supercapacitor, the p- and n- doped electrodes were separated using polypropylene separator soaked in the electrolyte. The performance of the so fabricated supercapacitor has been studied by cyclic voltammetry and AC Impedance spectroscopy with AUTOLAB 30.

Results and discussion

Cyclic voltammetry and FTIR spectroscopy

The electrodeposition of PEDOT on SS electrodes was carried out by cyclic voltammetry with 1 cm^2 SS electrodes in the electrolyte containing 0.1 M EDOT and 0.1 M Tetrabutyl ammonium perchlorate in acetonitrile that had been purged with nitrogen to remove dissolved oxygen. In all of the electrochemical studies voltammetric scans were terminated at the positive potential limit to ensure that within 500 cycles the electrodes get doped sufficiently.

Anionic doping or p- doping is a phenomenon wherein the oxidation caused by a chemical species generates a positively charged conducting polymer with an associated anion as depicted below which is relevant to the present study.

$$\text{PEDOT} + \text{ny}A^- \rightleftarrows [\text{PEDOT}]^{n+}A_y^- + \text{n}\,\text{y}e^-$$

For p-doping the electrode, cyclings (500 cycles) were done at a scan rate of 100 m Vs^{-1} by keeping the potential between 0 V to +1.2 V. Figure 1 shows the cyclic voltammogram (CV) for the electrodeposition of the p- doped PEDOT film on the SS electrode under cycling. The current increased from 50 to 200 cycles and reached a maximum at 500 cycles, ensuring the formation and growth of the p-doped PEDOT film on the SS electrode. Similarly for cationic doping or n- doping the electrode, cyclings (500 cycles) were done at a scan rate of 100 m Vs^{-1} by keeping the potential between 0 V to –1.5 V.

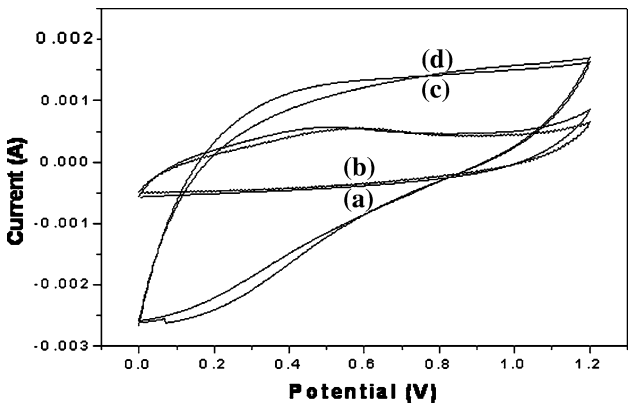

Fig. 1 CVs of P doping cycling in 0.1 M Tetrabutylammonium-perchlorate at (**a**) 50 cycles (**b**) 100 cycles (**c**) 150 cycles (**d**) 200 cycles

Further, FTIR Spectra of the p and n doped PEDOT on SS electrodes were taken to confirm the doping (Fig. 2). From the figure it can be seen that doping induced bands originating from the changes in the conjugated backbone due to the electron withdrawing and electron donating dopants on the polymer chain and counter ion balancing appear at 1090, 1470 and1423 cm^{-1} [11, 12]. The specific capacitance values of these p and n doped electrodes were calculated from the CV of these electrodes(not shown) in monomer free solution using the equation:

$$C = i/s$$

where 's' is the potential sweep rate and 'i' is the average current [13] are, 134 and 63 F g^{-1} respectively at a scan rate of 10 mV s^{-1}.

The cyclic voltammogram of n/p doped PEDOT supercapacior in 0.1 M Tetrabutyl ammonium perchlorate in acetonitrile is shown in Fig. 3, which is different from that for a typical electrical double layer capacitor, wherein a rectangular behavior is observed. However the CV observed here is similar to that reported for conducting polymer supercapacitors [14, 15]. The deviation from rectangular behavior may be due to the difference in the mechanism of charge storage action in the conducting polymer based supercapacitor compared to that in a double layer supercapacitor [16]. The specific capacitance calculated from the CV showed a maximum value of 121 F g^{-1} at a scan rate of 10 mV s^{-1}. This performance is much better than such supercapacitors fabricated based on n/p doped poly(dithieno(3,4-b;3′, 4′-d thiophene) [3, 17] n/p doped poly(3-methyl thiophene) [18–20], Poly (ethylenedioxythiophene)[21], Polypyrrole/Polyaniline [22, 23].

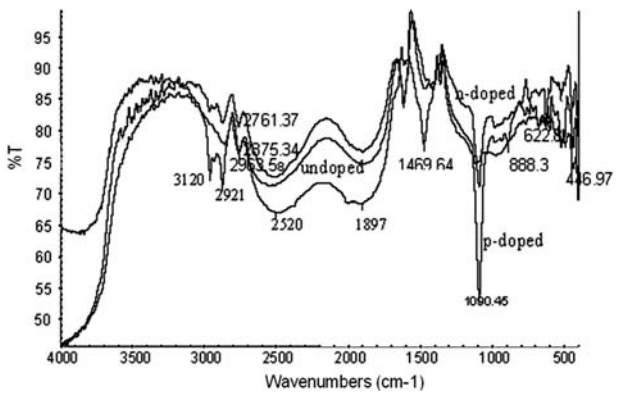

Fig. 2 FTIR Spectra of undoped and n/p doped PEDOT

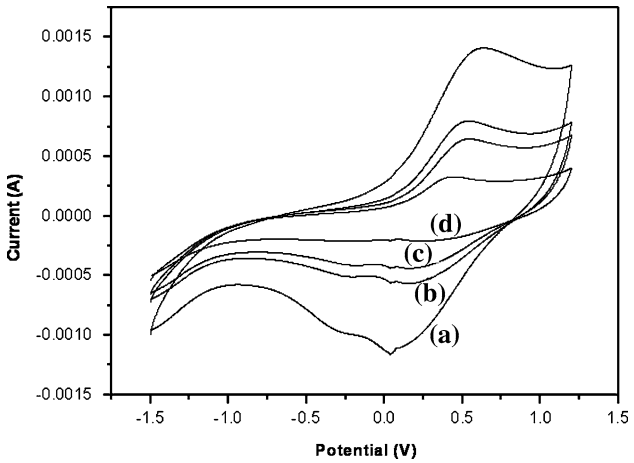

Fig. 3 CV of n/p Pedot supercapacitor in 0.1 M Tetrabutylammoniumperchlorate at scan rates of (**a**) 50 mV s^{-1} (**b**) 25 mV s^{-1} (**c**) 20 mV s^{-1} (**d**) 10 mV s^{-1}

AC Impedance spectroscopy

The AC impedance responses of the individual p doped PEDOT electrode in monomer free solution, at various cyclings are shown in Fig. 4. As is evident from the figure, formation of semicircles is observed at high frequencies in the range 1–10 kHz and an almost a straight line in the low frequency region. The capacitance value of the electrode increased at low frequencies due to a larger number of ions movement, which cause a decrease in the bulk resistance of the capacitor. The semi-circle results from the parallel combination of resistance and capacitance and the linear region is due to Warburg impedance [24]. Similar results were observed in the case of n doped PEDOT electrode in monomer free solution.

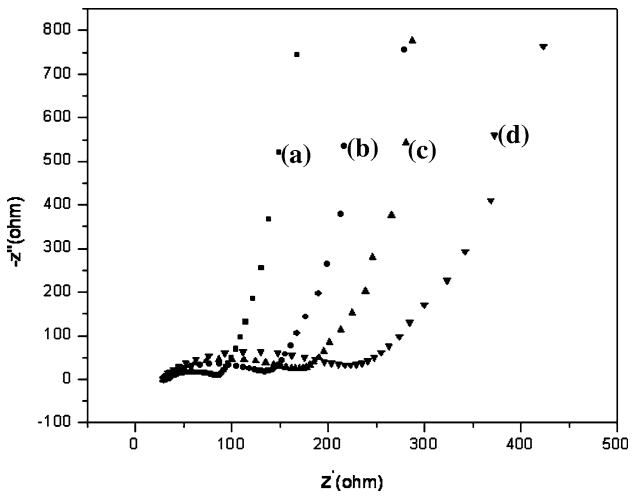

Fig. 4 Nyquist plot of p-doping cyclings (**a**) 100 cycles (**b**) 200 cycles (**c**) 300 cycles (**d**) 500 cycles

The impedance Nyquist plots for both the p (Fig. 5) and n doped electrodes (not shown) in monomer free solution show that at low frequency region, the linear part leans more towards imaginary axis, indicating a good capacitive behavior. The Nyquist plot of the n/p PEDOT supercapacitor (Fig. 6) also shows the similar behaviour. The capacitance, internal resistance and time constant are of importance for considering the capacitor performance. Supercapacitors generally oscillate between two states; resistive at high frequencies and capacitative at low frequencies. Between these two states it behaves like a resistance capacitance transmission line circuit [25–27]. At high frequencies, supercapacitors behave like a resistance.

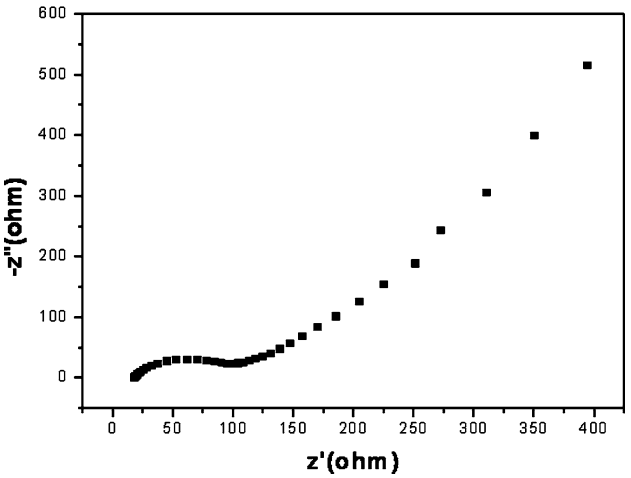

Fig. 5 Nyquist plot of p- doped electrode in 0.1 M Tetrabutylammoniumperchlorate in Acetonitrile

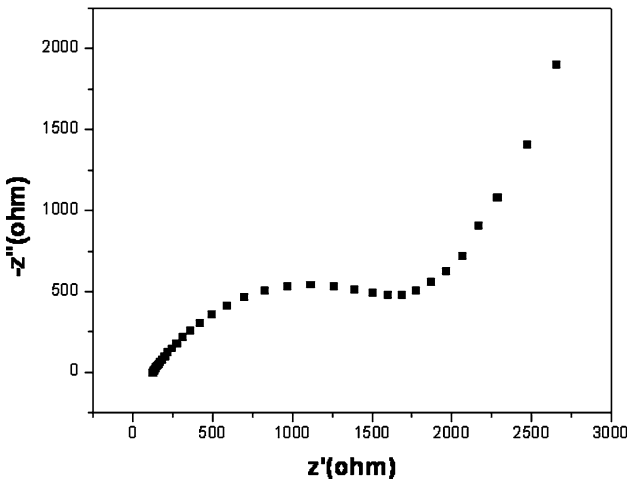

Fig. 6 Nyquist plot of n\p supercapacitor

At low frequency, the imaginary part of the impedance sharply increases and the plot tends to a vertical line characteristic of capacitive behavior. In the middle frequency range, the influence of electrode porosity and thickness on the migration rates of ions from the electrolyte inside the electrode can be seen [13, 17]. This shifts the low frequency capacitive behavior along the real axis toward more resistive values.

Figure 7 presents the normalized reactive power or imaginary part, |Q|/|S| and active power or real part |P|/|S| of the complex power versus frequency plot for the supercapacitor. The normalized active power corresponds to the power dissipated in the system. The impedance behaviour of the supercapacitor varies from a pure resistance at high frequency to pure capacitance at low frequency, as shown in Fig. 6. All the power is dissipated (P=100%) at high frequency, when the supercapacitor behaves like a pure resistance R as is seen in Fig. 7. The real part of the complex power P dissipated in a pure capacitance is zero and this is also observed in Fig. 7, where |P|/|S| decreases when frequency is decreased. It may be remembered here that the pure capacitance exhibits only reactive power Q. The maximum of |Q|/|S| is then reached at low frequency when the supercapacitor behaves like a pure capacitance. The crossing of the two plots appears when |P| = |Q|, that is when $\varphi = +45°$ and $|P|/|S| = |Q|/|S| = 1/\sqrt{2}$, corresponding to the time constant τ_o, defined as $\tau_o = 1/f_o$ where f_o is the frequency [13]. This time constant τ_o, which is also known as dielectric relaxation time has also been described as the characteristic feature of the system. Further, this plot provides information regarding the difference in the way to change from resistive to capacitive behavior of the system. The change occurs roughly from 5 kHz (resistive) down to 50 Hz (capacitive) i.e., over three orders of magnitude. Hence use of this capacitor can be achieved with high efficiency at low frequency region. The time constant for the solid state capacitor under study was calculated to be 1.2×10^{-2} s. The time constant τ_o, represents [13] a transition for the supercapacitor between a resistive behavior for frequency higher than $1/\tau_o$ and a capacitive behavior for frequencies lower than $1/\tau_o$, indicating that the present system can be efficiently used in the low frequency range up to around 100 Hz.

Charge–Discharge characterization

The conducting polymers used in type III capacitors are p- and n- doped one's functioning as the positive and the negative electrodes respectively. When the capacitor is charged, the positive electrode is fully p-doped and the negative electrode is fully n-doped. The p- and n- doping sources come from the electrolyte, such as cations of Bu_4N^+ and anions of ClO_4^-. These doping charges are released on discharge [28]. When the cell is fully discharged, both electrodes end up in their undoped state. Therefore, for pseudocapacitors with type III conducting polymer electrodes, the salt concentration in the electrolyte changes during the charge and the discharge.

The overall reaction is as follows

$$\text{PEDOT} + C^+A^- \rightleftarrows \text{PEDOT}//A^- + \text{PEDOT}//C^+$$

Figure 8 presents the charge discharge curves of the fabricated supercapacitor at a constant current density of 3 mA cm^{-2} at different cycles between 0 and 1.0 V. It is seen that the initial voltage drop during discharge is negligibly small and the voltage of the capacitor varies almost linearly with time during both charging and discharging processes for various cycles. The charging time and also discharging time decreased with increase of cycles as well

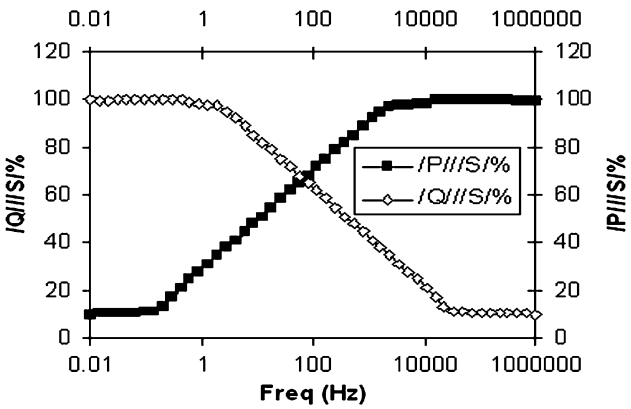

Fig. 7 Normalized reactive power|Q|/|S|% and active power |P|/|S|% vs. frequency (Hz) plot for the 1 cm^2 cell n/p Edot supercapcacitor

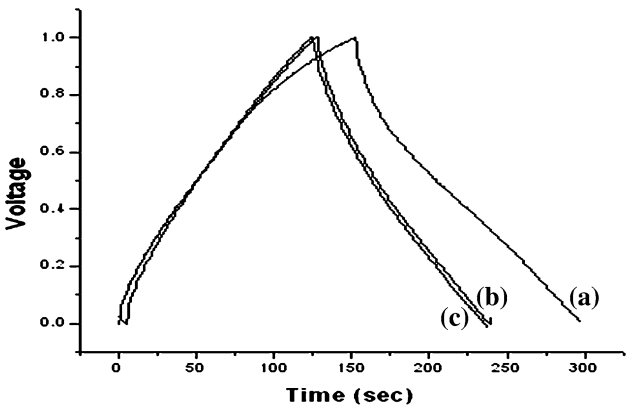

Fig. 8 Galvanostatic charge-discharge curves of n/p PEDOT supercapacitor at a constant current density of 3 $mAcm^{-2}$ (**a**) Ist cycle (**b**) 1000th cycle (**c**) 5000th cycle

as with current density. However, the efficiency of charge–discharge cyclings is high in the range of 98–99%.

Conclusion

A symmetric redox supercapacitor based on n/p doped Poly(3,4-ethylenedioxythiophene) has been fabricated and studied for the first time. The performance evaluation study reveals that n/p doped PEDOT electrode can be successfully prepared and are suitable for the fabrication of a supercapacitor. The capacitance value of the fabricated supercapacitor is much higher than such other supercapacitors reported. The supercapacitor can be used efficiently up to around 100 Hz and hence more suited for the low frequency range applications.

Acknowledgements The financial support in the form of an Institute Research Fellowship to MSK from National Institute of Technology Karnataka Surathkal is gratefully acknowledged.

References

1. Rudge A, Davey J, Raistrick I, Gottesfeld S, Ferraris JP (1994) J Power Sources 47:89
2. Rudge A, Davey J, Raistrick I, Gottesfeld S, Ferraris JP (1994) Electrochim Acta 39:273
3. Arbizzani C, Castellani M, Mastragostino M, Mingazzini C (1995) Electrochim Acta 40(12):1871
4. Ryu KS, Lee Y, Han K-S, Park YJ, Kang MG, Park N-G, Chang SH (2004) Solid State Ionics 175:765
5. Rudge A, Davey J, Raistrick I, Gottesfeld S, Ferraris JP (1993) Proc Electrochem Soc 93:74
6. Arbizzani C, Mastragostino M, Scrosati B (1997) In: Nalwa HS (ed) Handbook of organic conductive molecules and polymers. John Wiley and Sons
7. Sato M, Tanaka S, Kaeriyama K (1987) J Chem Soc Chem Comm 1725
8. Kaeriyama K, Tanaka S, Sato M, Hamada K (1989) Synth Metals 28:C611
9. Sato M, Tanaka S, Kaeriyama K (1989) Makromol Chem 190:1233
10. Roncali J, Yousuffi HK, Garreau R, Garnier F, Lemaire M (1990) J Chem Soc Chem Comm 414
11. Seo KI, Chung IJ (2004) Polymer 41(12):4491
12. Tran-Van F, Garreau S, Louarn G, Froyer G, Chevrot C (2001) J Mater Chem 11:1378
13. Taberna PL, Simon P, Fauvarque JF (2003) J Electrochem Soc 150(3):A292
14. Rajendra Prasad K, Munichandraiah N (2002) Electrochem Solid State Lett 5(12):A271–A274
15. Muthulakshmi B, Kalpana D, Pitchumani S, Renganathan NG (2006) J Power Sources 158:1533
16. Conway BE, Pell WG (2003) J Solid State Electrochem 7:637
17. Arbizzani C, Mastragostino M, Meneghello L (1995) Electrochim Acta 40(13&14):2223
18. Arbizzani C, Mastragostino M, Soavi F (2001) J Power Sources 100:164
19. Mastragostino M, Arbizzani C, Soavi F (2001) J Power Sources 97&98:812
20. Mastragostino M, Arbizzani C, Soavi F (2002) Solid State Ionics 148:493
21. Ryu KS, Lee Y-G, Hong Y-S, Park YJ, Wu X, Kim KM, Kang MG, Park N-G, Soon Ho Chang (2004) Electrochim Acta 50:843
22. Clemete A, Panero S, Spila E, Scrosati B (1996) Solid State Ionics 85:273
23. Ryu KS, Kim KM, Park N-G, Park YJ, Chang SH (2002) J Power Sources 103:305
24. Conway BE (1999) Electrochemical supercapacitors: scientific fundamentals and technological applications. Kluwer academic publishers, Plenum press, New York
25. Qu D, Shi H (1998) J Power Sources 74:99
26. Song HK, Jung YH, Lee KH, Dao LH (1999) Electrochim Acta 44:3513
27. Keiser H, Beccu KD, Gutjahr MA (1976) Electrochim Acta 12:539
28. Zheng JP, Huang J, Jow TR (1997) J Electrochem Soc 144(6):2026